QUANTITATIVE THERMAL WAVE CHARACTERIZATION OF COATING ADHESION DEFECTS

J. Jaarinen[1], J. Hartikainen, and M. Luukkala
University of Helsinki
Department of Physics
Siltavuorenpenger 20 D
SF-00170 Helsinki
Finland

INTRODUCTION

Throughout the development of thermal wave NDE techniques the most common application has been the imaging of subsurface structure of coated and bulk materials [1]. The use of thermal wave imaging for the detection of coating adhesion defects was first proposed by Luukkala and Penttinen [2], and Busse and Ograbek presented the first experimental results on the detection of artificial adhesion defects of a graphite coating on aluminum [3].

The thermal wave evaluation of plasma sprayed coatings has been of interest in the recent years [4-8]. There are very few NDT methods available to characterize the quality of these coatings. Only visual inspection and Eddy-current thickness measurement are commonly used. Ultrasonic techniques do not work well because of the heterogeneous structure of these coatings [9], which causes adverse scattering of the sound waves. Thermal waves offer a totally noncontacting and nondestructive method. The microstructure contributes to the propagation of thermal waves only through the macroscopic thermal diffusivity of the coating material.

In this work we present one-dimensional analysis of thermal wave propagation in a coated sample with an adhesion defect. The adhesion defect is described in terms of thermal contact resistance. The optimization of the adhesion defect detection will be discussed. The presented method is applied to the quantitative characterization of adhesion defects of a plasma sprayed ceramic coating.

---

1 Present address Neste Oy, Technology Centre, SF-06850 Kulloo, Finland

THEORY

The quantity that is used for the characterization of a defective interface between the coating and the substrate is thermal contact resistance, R_{bd}, which is defined as the ratio of the temperature discontinuity, T_1-T_2, and the heat flux, ϕ, through the interface. The subscript 1 refers to the coating and 2 to the substrate. The boundary condition for the temperature at the coating/substrate interface is then

$$T_1-T_2 = R_{bd}\,\phi. \qquad (1)$$

The heat flux is continuous at the interface because the defect does not cause any heat to accumulate at the interface.

The one-dimensional reflection coefficient of thermal waves in the presence of thermal contact resistance can be obtained by applying Eq. (1) and the continuity of the heat flux to a propagating thermal plane wave. The result can be written as

$$S_d = \frac{1-\dfrac{e_2}{e_1}+\dfrac{(1+j)}{\sqrt{2}}e_2\,R_{bd}\sqrt{\omega}}{1+\dfrac{e_2}{e_1}+\dfrac{(1+j)}{\sqrt{2}}e_2\,R_{bd}\sqrt{\omega}}\,. \qquad (2)$$

In Eq. (2) e is the thermal effusivity of the material, $e = (KC)^{-1/2}$, where K is the thermal conductivity and C the heat capacity per unit volume. The effect of non-zero thermal contact resistance on the reflected wave is through the last term in both the numerator and denominator. The reflection coefficient is frequency dependent and also complex, which is in contrast to the case of a thermally good interface ($R_{bd} = 0$). Because of the frequency dependence of the magnitude and phase of the reflected wave, frequency is an essential parameter in optimization of the detection of coating adhesion defects.

The behavior of the real and imaginary part of the reflection coefficient at a plasma sprayed chromium oxide coating on a steel substrate is illustrated in Fig. 1 as a function of $R_{bd}\sqrt{\omega}$. The real part increases monotonically from the value of the ideal interface to one at high frequencies and large thermal contact resistances. The imaginary part is negligible at low and high values of $R_{bd}\sqrt{\omega}$ and has a maximum of 0.33 when $R_{bd}\sqrt{\omega} \sim 4\times10^{-4}\ Km^2W^{-1}s^{-1/2}$.

The measurable quantities in thermal wave imaging are the magnitude and phase of the thermal wave on the surface of the coating. The total wave, $\tau_s(0,t)$, at the surface can be found out by solving the heat diffusion equation with the boundary condition in Eq. (1) [10]

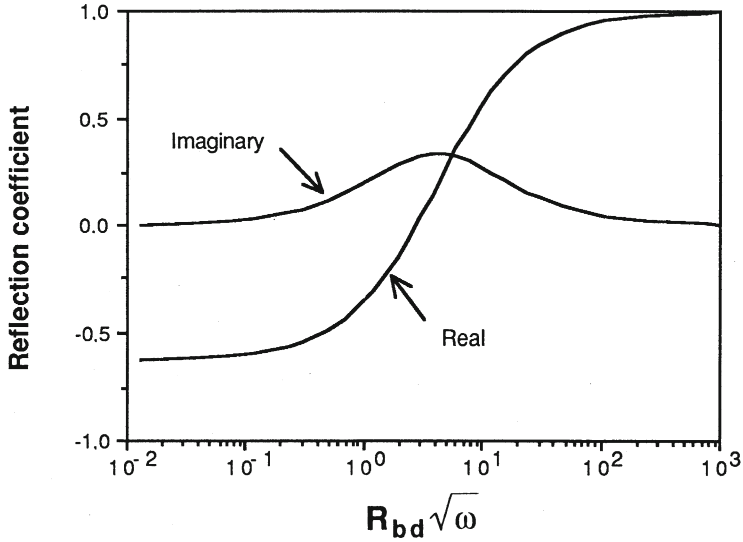

Figure 1. The real and imaginary part of the reflection coefficient, Eq. (2), at the interface of the Cr_2O_3 plasma sprayed coating and steel (e_1=3.0x10^3 Ws$^{1/2}$K^{-1}m^{-2} and e_2 =1.3x10^4 Ws$^{1/2}$K^{-1}m^{-2}). The horizontal axis is the product of the thermal contact resistance and the square root of the thermal-wave angular frequency (in Kcm^{2}W^{-1}s$^{-1/2}$).

$$\tau_s(0,t) = \frac{I_o}{4K_1\sigma_1} \frac{1+ S_d e^{-2\sigma_1 l}}{1- S_d e^{-2\sigma_1 l}} e^{j\omega t} , \qquad (3)$$

where $\sigma = (1+j)/\mu$ is the complex wave vector of the thermal wave. The thickness of the coating is abbreviated as l and I_o is the intensity of the heating. The ratio of the thickness to the thermal diffusion length, l/μ is the normalized thickness of the coating. In Eq. (3) has been approximated that the coating is opaque. Fig 2. presents the relative magnitude and the phase shift of the thermal wave on the surface of the sample of Fig. 1.

The behavior of the magnitude and phase of the thermal wave at the surface of the Cr_2O_3/steel sample as a function of frequency is presented in Fig. 3. The curves represent the relative magnitude and the phase change of the detectable thermal wave on the surface of the coating at several different values of thermal contact resistance ranging from 3.0x10^{-6} Km^{2}W^{-1} to 1.0x10^{-3} Km^{2}W^{-1}. The curves are calculated from Eq. (12). The damping of the reflected wave causes the changes to level off when the frequency exceeds 20 Hz. The corresponding the normalized thickness of the coating is 2.1. At very low frequencies the changes in the magnitude and phase signal also level off when the thermal contact resistance is small, as can be expected on the basis of Eq. (2).

As seen in Fig. 2a the largest changes in the magnitude signal occur at frequencies lower than 1 Hz. However, these frequencies are impractical for experimental work. The detection methods do not work well below 1 Hz when the usual lock-in analyzer technique is used [11], and also the measurement time increases in scanning experiments, because the balancing of the signal takes a few heating cycles at each measurement point [12].

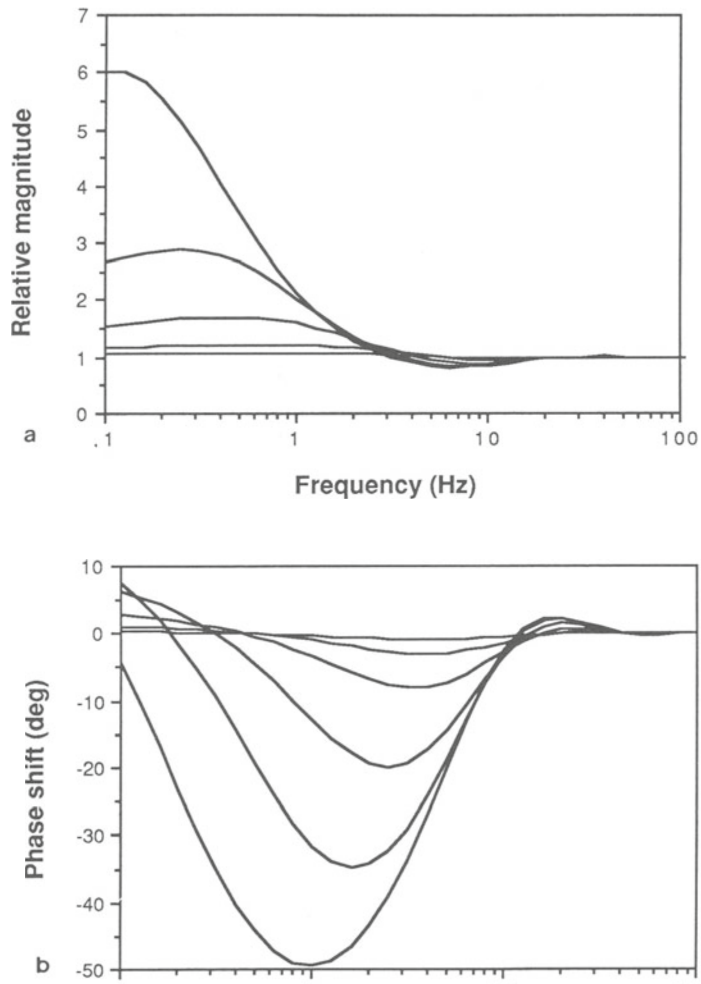

Figure 2. The relative magnitude (a) and phase shift (b) of thermal waves at the surface of the plasma sprayed coating as a function of frequency. The thickness of the coating was 0.2 mm. The set of curves represents thermal contact resistances of 0.03, 0.1, 0.3, 1.0, 3.0, and 10×10^{-4} Km^2W^{-1} in both pictures. The largest relative magnitude and the largest phase shift were caused by the largest thermal contact resistance.

Fig. 2b shows the phase shift of the coating surface thermal wave caused by defective adhesion. The phase difference has a maximum value, whose magnitude and position depend on the thermal contact resistance. The smaller the contact resistance is, the smaller the maximum phase change is and the higher the corresponding frequency. Thus the optimum detection frequency depends on the severity of the defect.

The optimization of the adhesion-defect detection can be achieved by choosing the experimental parameters in such a way that all those defects can be found, which change the signal more than the average signal variation due to noise and normal structural inhomogenities of the sample do.

To optimize the detection of adhesion defects the measurement frequency should be chosen in such a way that the locations where the coating/substrate interface is only slightly defective cause the maximum phase shift. A good frequency in the case of Fig. 2 would be 3 Hz, because the a defect, whose thermal contact resistance is 1×10^{-5} Km^2W^{-1} causes its maximum phase shift at this frequency. It is to be noted that severe defects cause large phase shifts also at this frequency thus being detected for sure. At 3 Hz the normalized thickness of the coating is 0.8 thermal diffusion lengths.

EXPERIMENTAL

The comparison of the one-dimensional theory to experiments was carried out by studying a ring shaped plasma sprayed sample. The device used was an automated scanning photothermal microscope. The sample was heated with an square wave intensity modulated Ar-ion laser beam. The power of the focussed (300 μm) beam was about 100 mW. The thermal wave on the surface of the sample was detected by a partially focussed pyroelectric infrared detector (Plessey PLL255), and the magnitude and phase measured using a lock-in analyser (SRS530). The sample was scanned by a computer controlled steppingmotor xy-table made in our laboratory.

The sample was a waterpipe seal ring with a 0.2 mm thick plasma sprayed Cr_2O_3-coating on a steel substrate. The inner diameter of the washer shaped ring was 90 mm and the width of the coated surface 11 mm. During the preparation of the sample six areas of poor coating adhesion were produced by using protective coating against sand blasting, which is a standard preparation technique for the substrate prior coating in order to increase the coating adhesion [9]. The areas were 0.2 mm wide radial stripes extending from edge to edge (11 mm) in the sample.

All the areas have shown existence of weak adhesion in a previous study [6]. In this work the six positions were area scanned at four frequencies: 1, 3, 5, and 10 Hz. The distance between the measured points were either 0.3 or 0.5 mm. In all cases the entire areas of lacking surface preparation were found to be defective. The changes in magnitude and phase signals were detected at these locations. No other locations showed any traces of weakened adhesion in this sample.

In Fig. 3 is shown the phase signal of one of the defects at 5 Hz with an optical picture of the same area. The phase shift is increased near the edges of the sample due to the edge effect [13] and the cracking of the coating that can be seen at the top of optical picture. In Fig. 4 are presented the measured magnitude and phase signals along the center line of the defect. The arrows indicate, the locations were the signals were compared by direct graphical comparison with the calculated curves. The thermal parameters that were adjusted to give the best fit were $K_1=2.3$ $WK^{-1}m^{-1}$ and $e_2=1.3\times10^4$ $Ws^{1/2}K^{-1}m^{-2}$. The literature value 4.0×10^6 $Jm^{-3}K^{-1}$ was used for the heat capacity of the coating [14], thus the corresponding effusivity of the coating was 3.0×10^3 $Ws^{1/2}K^{-1}m^{-2}$. At location (a) thermal

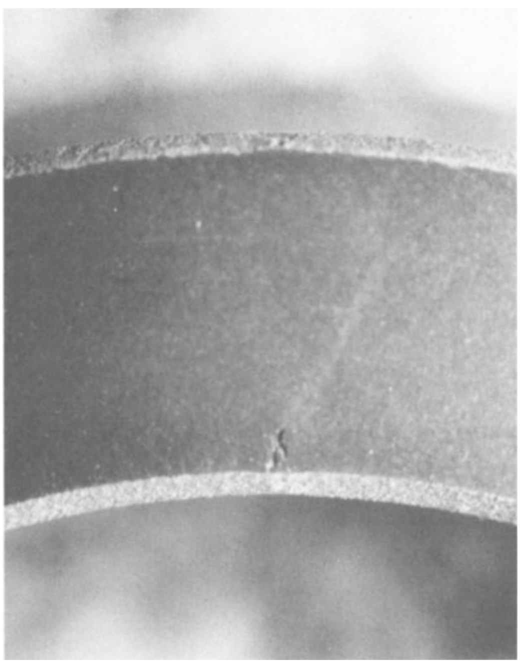

Figure 3. On the right is the phase scan over one of the defects at 5 Hz. The arrows point at the locations at which the measured magnitude and phase is compared with the theory. The comparison is presented in Fig. 4. On the left is an optical picture of the same area.

contact resistance was 1.7×10^{-5} Km^2W^{-1} and at (b) 3.9×10^{-5} Km^2W^{-1}. A microscopic study of the cross-section of the defective area showed that the coating is not delaminated, i.e. no air gap between the coating and the substrate exists [15].

The comparison of the experiments with the one-dimensional theory shows that in the case of the plasma sprayed coatings the weak adhesion of the coating can be associated with the thermal contact resistance. In cases when the size of the defective area is large enough the one-dimensional theory can be used for the quantitative determination of the thermal contact resistance. The results obtained here are similar to the results obtained by Patel *et.al.* [8].

The association of the thermal contact resistance and the strength of the adhesion seems to be very material dependent. Egee *et. al.* were not able to detect the weak adhesion of enamel coatings [10]. Similar results have been obtained by Jaarinen *et. al.* when bonding of thin copper films were studied [16]. When thermal wave microscopy is used for the evaluation of coating adhesion the correlation of the thermal contact resistance and the strength of the adhesion is to be determined separately for each coating/substrate combination.

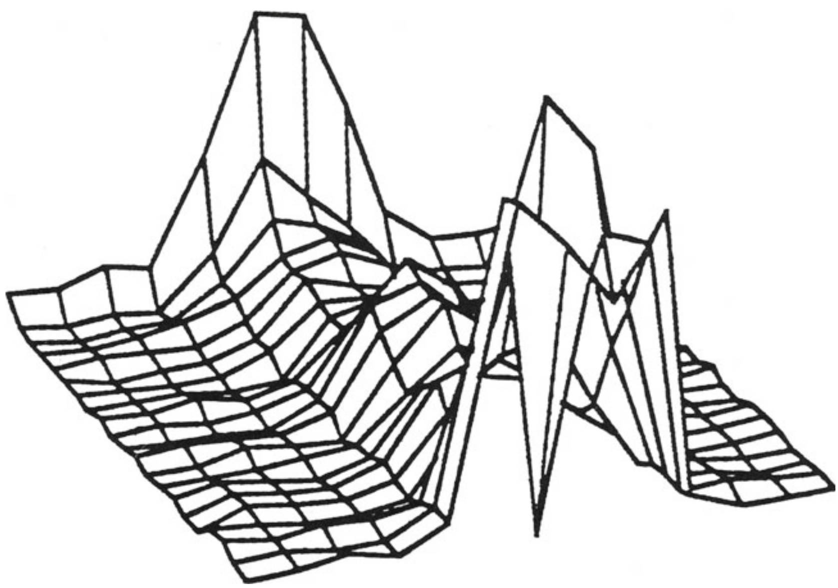

Defect 6

Figure 3. (right)

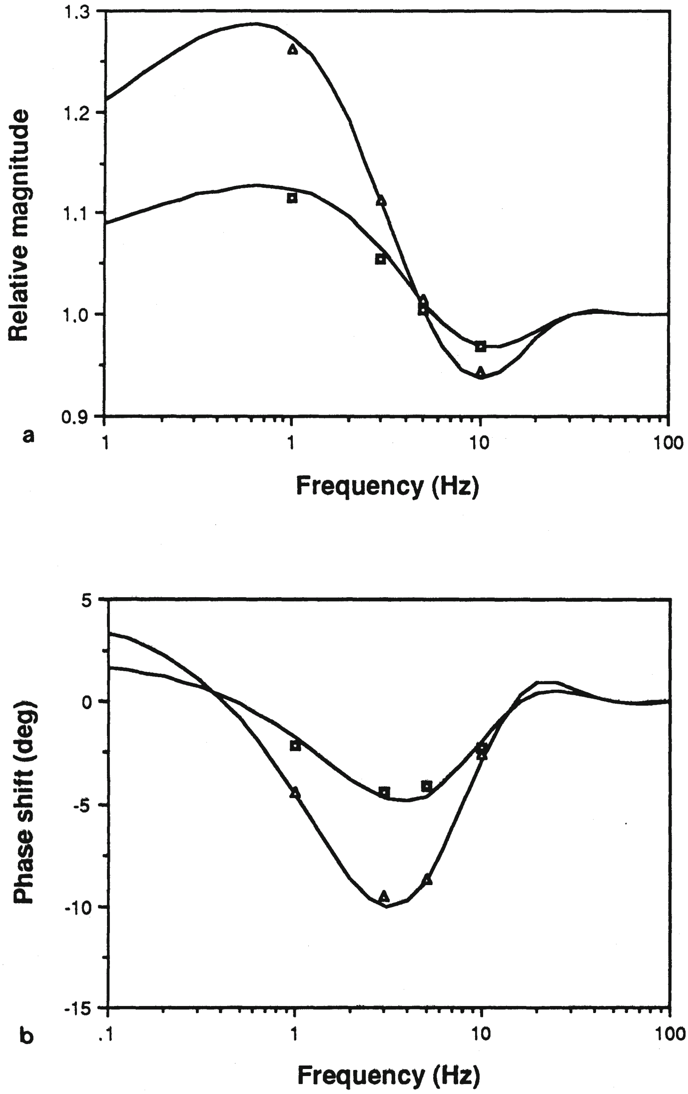

Figure 4. Comparison between the experimental results at the two locations indicated by arrows in Fig. 11 and the one-dimensional theory in Eq. (12).

ACKNOWLEDGEMENTS

This work was supported by The Technology Development Centre of Finland.

REFERENCES

1. G Busse, IEEE Trans. Son. Ultrason., SU-32, 355-364, 1985
2. M. Luukkala and A. Penttinen, Electron. Lett., 15, 325-326, 1979
3. G. Busse and A. Ograbek, J. Appl. Phys, 51, 3576-3578, 1980
4. A. Lehto, M. Jokinen, J. Jaarinen, T. Tiusanen, and M. Luukkala, Electron. Lett., 17, 540-541, 1981
5. D.P. Almond, P.M. Patel, and H. Reiter, J. Phys. Colloq., 44, 491-495, 1983
6. J. Jaarinen and M. Luukkala, Proceedings of The Third European Conference on Nondestructive Testing, vol. 5, Oct 15-18, Firenze, Italy, 128-138, 1984
7. P.M. Patel and D.P. Almond, J. Mat. Sci., 20, 955-966, 1985
8. P.M. Patel, D.P. Almond, and H. Reiter, Appl. Phys., B43, 19-15, 1987
9. J.H. Zaat, Ann. Rew. Mat. Sci., 13, 9-42, 1983
10. M. Egee, R. Dartois, J. Marx, and C. Bissieux, J. Can. Phys., 64, 1297-1302, 1986
11. L.D. Favro, P.K. Kuo, and R.L. Thomas, in Review of Progress in Quantitative Nondestructive Evaluation, vol.6A, D. O. Thompson and D. E. Chimenti, Eds., Plenum Press, New York 1987, 293-299
12. B. Rief, Can. J. Phys., 64, 1303-1306, 1986
13. F.A. McDonald, Three-dimensional heat flow in the photo-acoustic effect, Appl. Phys. Lett, 36, 123-125, 1980
14. CRC Handbook in Chemistry and Physics, 67th Edition, CRC Press, Boca Raton, Florida, 1986
15. J. Jaarinen, Nondestructive Evaluation of Coatings by Low-Frequency Thermal Waves, PhD Thesis, Acta Polytechnica Scandinavica, Appl. Phys. Series, No. 162, The Finnish Academy of Technology, Helsinki 1988
16. J. Jaarinen, C.B. Reyes, I.C. Oppenheim, L.D. Favro, P. K. Kuo, and R.L. Thomas, in Review of Progress in Quantitative Nondestructive Evaluation, vol. 6B, D.O. Thompson and D. E. Chimenti, Eds., Plenum Press, New York 1987, 1347-1352